

HCl Quasi-Biennial Oscillation in the Stratosphere and a Comparison with Ozone QBO

CHEN Yuejuan^{*1} (陈月娟), SHI Chunhua¹ (施春华), and ZHENG Bin² (郑彬)

¹*School of Earth and Space Sciences, University of Science and Technology of China, Hefei 230026*

²*Institute of Tropical and Marine Meteorology, China Meteorological Administration, Guangzhou 510080*

(Received 16 December 2004; revised 31 March 2005)

ABSTRACT

HALOE data from 1992 to 2003 are used to analyze the interannual variation of the HCl volume mixing ratio and its quasi-biennial oscillation (QBO) in the stratosphere, and the results are compared with the ozone QBO. Then, the NCAR two-dimensional interactive chemical, dynamical and radiative model is used to study the effects of the wind QBO on the distribution and variation of HCl in the stratosphere. The results show that the QBO signals in the HCl mixing ratio are mainly at altitudes from 50 hPa to 5 hPa; the larger amplitudes are located between 30 hPa and 10 hPa; a higher HCl mixing ratio usually corresponds to the westerly phase of the wind QBO and a lower HCl mixing ratio usually corresponds to the easterly phase of the wind QBO in a level near 20 hPa and below. In the layer near 10 hPa–5 hPa, the phase of the HCl QBO reverses earlier than the phase of the wind QBO; the QBO signals for HCl in the extratropics are also clear, but with reversed phase compared with those over the Tropics. The HCl QBO signals at 30°N are clearer than those at 30°S; the QBOs for HCl and ozone have a similar phase at the 50 hPa–20 hPa level while they are out of phase near 10 hPa; the simulated structures of the HCl QBO agree well with observations. The mechanism for the formation of the HCl QBO and the reason for differences in the vertical structure of the HCl and ozone QBO are attributed to the transport of HCl and ozone by the wind QBO-induced meridional circulation.

Key words: HCl, quasi-biennial oscillation, stratosphere

1. Introduction

The quasi-biennial oscillation (QBO) of the mean zonal wind in the equatorial stratosphere was discovered by Reed et al. (1961) and Verryard and Ebdon (1961). Later, Funk and Garnham (1962) and Ramanathan (1963) were the first to describe the ozone QBO and they showed that it correlated with the QBO in the zonal wind. More observations (Zawodny and McCormick, 1991; Schoeberl et al., 1997 and Luo et al., 1997) and modeling studies (Gray and Chipperfield, 1990; Gray and Ruth, 1992; Chipperfield et al., 1994; Zhang et al., 2000) showed that the long-lived tracers in the tropical stratosphere exhibit obvious QBO characteristics. The QBOs in HCl, HF, CH₄, and H₂O were first reported by Luo et al. (1997) and although only 4 years of observed data were used in their paper, the QBO signal in the HCl mixing ratio is noticeable. In this paper, we will use longer term HALOE data to discuss the vertical structure

of HCl QBO in the Tropics, the HCl QBO signals in the extratropics and the comparison of the HCl and ozone QBO. We will then discuss results of simulations using the National Center for Atmospheric Research (NCAR) two-dimensional interactive chemical, radiative and dynamical model.

2. Results from observations

The HCl and O₃ volume mixing ratio data used in this work are given by the Halogen Occultation Experiment (HALOE) observations from 1992 to 2003. The Halogen Occultation Experiment was launched on the Upper Air Research Satellite (UARS) spacecraft, which uses the principle of satellite solar occultation to measure vertical profiles of O₃, HCl, HF, CH₄, H₂O, NO, NO₂, aerosol extinction and temperature. The latitude coverage is from 80°S to 80°N with a slight seasonal change and the vertical range is from 5 km to ~60–130 km with 271 levels vertically. The

*E-mail: cyj@ustc.edu.cn

HALOE instrument includes both broadband and gas filter channels. The broadband radiometer is used to measure O_3 , H_2O and NO_2 , while the gas filter radiometry is used for HCl, HF, CH_4 and NO. More detailed descriptions of the instrument and the measurement approach can be found in Russell (1993). The zonal wind data come from National Centers for Environmental Prediction (NCEP) reanalyzed data.

2.1 Characteristics of HCl QBO over the Tropics

The altitude-time cross section for the zonal mean HCl mixing ratio anomaly over the Tropics ($10^\circ S$ – $10^\circ N$) is shown in Fig. 1a. It is clear that the QBO signals in HCl mixing ratio are strongest in the altitude range from 50 hPa to 5 hPa: The larger amplitudes are located between 30 hPa to 10 hPa, with the value of the amplitudes being about 0.2 ppbv to 0.05 ppbv.

Figure 1b gives the altitude-time cross section for the zonal wind over the equator, which was obtained

from NCEP reanalyzed data. Comparing Figs. 1a and 1b, we can see the relationship between the HCl and the zonal wind QBO signature. When the westerly phase of the wind QBO is dominant near 20 hPa, the HCl mixing ratio is higher than normal at this level, and when the easterly phase of the wind QBO is dominant near 20 hPa, the HCl mixing ratio is lower. The phase of the HCl QBO reverses earlier than the phase of the wind QBO in the layer around 10 hPa to 5 hPa.

Figure 1c shows the altitude-time cross section for the ozone mixing ratio anomaly over the Tropics ($10^\circ S$ – $10^\circ N$). It can be seen from Figs. 1a and c that the vertical structure of the ozone QBO over the Tropics is more complex than that for HCl. As indicated by Chen et al. (2002), the phase of the ozone QBO changes many times with height in the Tropics. Changes in the HCl QBO phase are less variable, and in the lower stratosphere, the phase is usually opposite to the one in the upper levels.

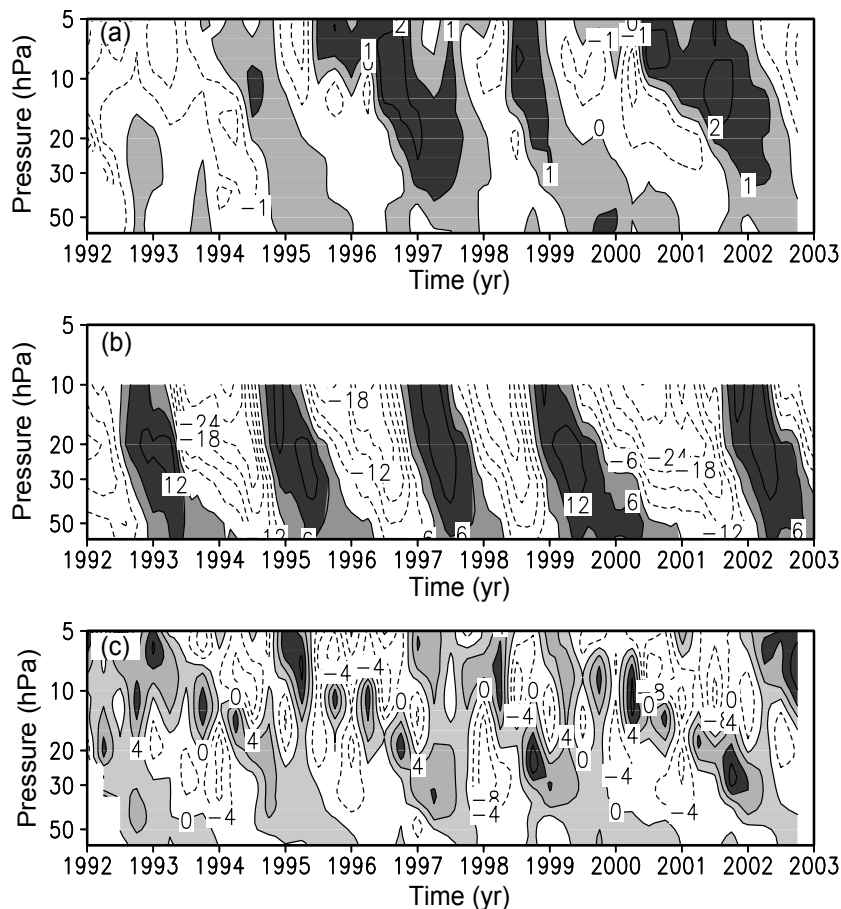


Fig. 1. Pressure versus time cross section for the anomalies of (a) HCl mixing ratio (units: 0.1 ppbv), (b) zonal wind (units: $m s^{-1}$) and (c) O_3 mixing ratio (units: 0.1 ppmv) over the Tropics.

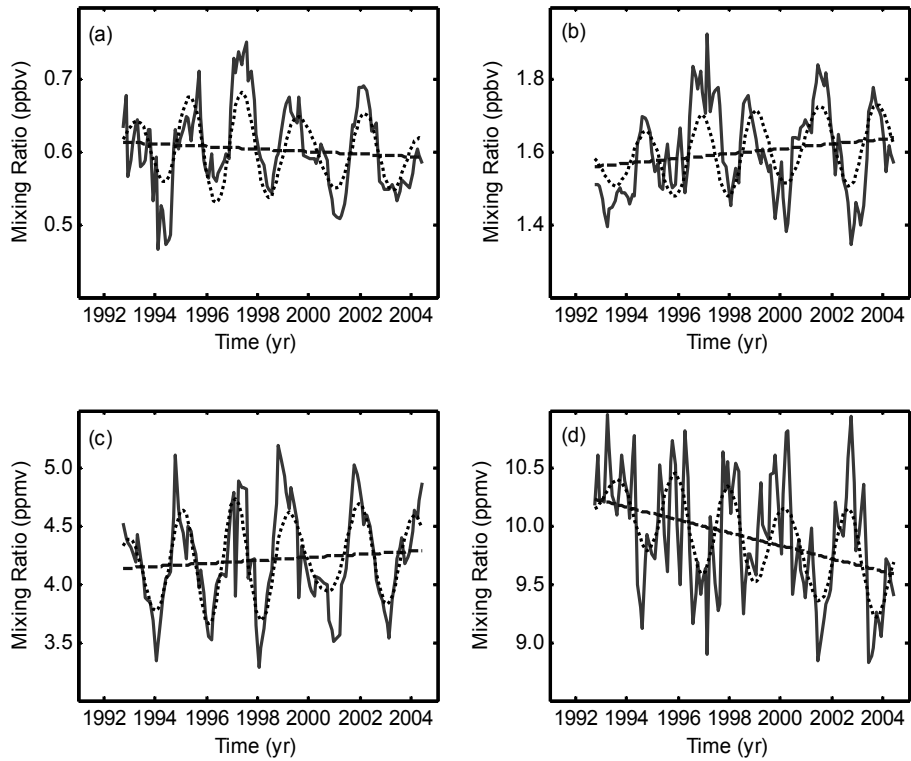


Fig. 2. Time series for HCl and ozone mixing ratios over the Tropics (10°S–10°N). (a) HCl, 29.3 hPa; (b) HCl, 10.0 hPa; (c) O₃, 29.3 hPa; (d) O₃, 10.0 hPa.

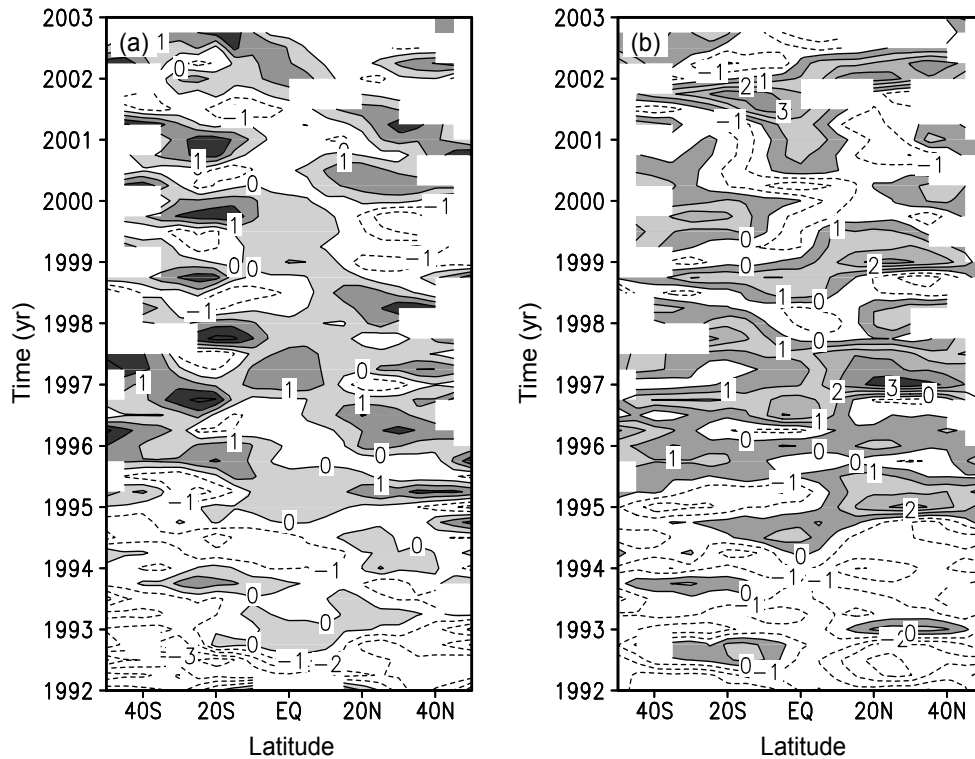


Fig. 3. The HCl mixing ratio anomaly time-latitude cross section (units: 0.1 ppbv). (a) 29.3 hPa; (b) 10.0 hPa.

The HCl and ozone mixing ratio time series for 29.3 hPa and 10.0 hPa over the Tropics (10°S – 10°N) are shown in Fig. 2. In Fig. 2, the solid curves are the zonal averaged mixing ratios over the Tropics. We can see the signals of the QBO and semiannual oscillation (SAO) for HCl and O_3 at these two pressures. The SAO signals for both HCl and O_3 in the middle stratosphere are much stronger than those at the lower level. The dashed lines in Fig. 2 are the linear time trends, which show that the HCl mixing ratio increased and the O_3 mixing ratio decreased obviously with time at the 10 hPa level, while near 29.3 hPa the HCl mixing ratio decreased slightly in the last 10 years, and the O_3 mixing ratio increased somewhat at this level. In order to obtain the QBO signals, the band-pass filter method was used, i.e., Fourier analyses were carried out for the dataset and then filtered to remove the oscillations with periods shorter than 20 months and longer than 36 months. The dotted curves in Fig. 2 show the oscillations in the HCl and O_3 mixing ratios with periods longer than 20 months or shorter than 36 months. From the dotted curves we can see signals of the QBO for HCl and O_3 more clearly at the two pressures. We can also see that the phase of the HCl QBO in the lower stratosphere (~ 30 hPa) is usually opposite to that in the upper layer (~ 10 hPa); the HCl and O_3 QBO are in phase near the 30 hPa level while they are

out of phase at 10 hPa.

2.2 The HCl QBO signals over the extratropics

Similar to the ozone QBO (Hasbe, 1983; Yang and Tung, 1995), the HCl QBO signal exists not only over the Tropics but also over the extratropics. Figures 3a and 3b show the time-latitude cross sections of the zonal mean HCl mixing ratio anomaly at 29.3 hPa and 10 hPa, respectively. We can see the oscillation in both the northern and southern hemispheric extratropics, but with reversed phase compared with that in the Tropics. The phases reverse near 12°N/S latitude and show a hemispheric asymmetry.

Figure 4 shows the HCl mixing ratio time series for 29.3 hPa and 10 hPa for 30°N and 30°S , respectively. The dotted curves in the figure show the signals of the HCl QBO, which were obtained by using the same method as for Fig. 2. It can be seen that the signal of the HCl QBO at 30°N is stronger than that at 30°S , and the QBO signals at 10 hPa are stronger than at 29.3 hPa. The solid curves (zonal averaged HCl mixing ratio) in the figure show the annual and semiannual oscillations which appear to be strongest at 30°S and 10 hPa. The dashed curves also show that the HCl mixing ratio increases with time for both latitudes and pressure levels.

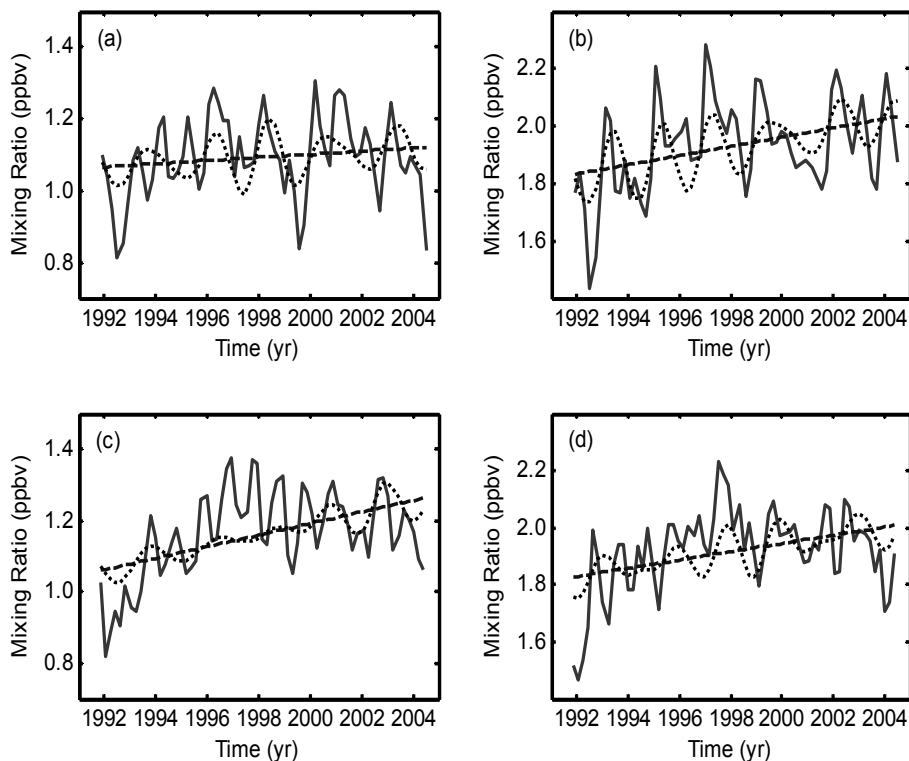


Fig. 4. HCl mixing ratio time series for 30°N and 30°S . (a) 30°N , 29.3 hPa; (b) 30°N , 10.0 hPa; (c) 30°S , 29.3 hPa; (d) 30°S , 10.0 hPa.

3. Simulations results

The model used in the numerical experiment is the NCAR two-dimensional interactive chemical, radiative and dynamical model (SOCRATES) (Huang et al. 1997). The parameterized method for the wind QBO forcing is described in Chen et al. (2002). Our simulation was carried out for 6 model years. The wind QBO given by the model and the simulated HCl zonal mean anomaly (difference of HCl mixing ratio between the simulation with the wind QBO and that without the wind QBO) are shown in Figs. 5a and 5b, respectively.

It is clear that the wind QBO leads to an HCl QBO, and the phases of the HCl QBO over the equator are almost the same as the wind QBO in the layer below 20 hPa. That is, when the westerly phase of the wind QBO dominates, the simulated HCl mixing ratio over the equator is higher than that simulated without the wind QBO, and when the easterly phase of the wind QBO dominates, the simulated HCl mixing ratio over

the equator is lower. In the layer above 20 hPa, the phase reversal of the HCl QBO shifts to an earlier date than that of the wind QBO. Figure 5c is the simulated O_3 anomaly over the equator (difference of the O_3 mixing ratio between the simulation with the wind QBO and that without the wind QBO). It is clear that with the same wind QBO forcing, the simulated vertical structures for the HCl and O_3 QBOs are very different. However they agree well with the observations shown in Fig. 1.

In order to study how the wind QBO leads to the HCl QBO over the Tropics and extra tropics, we examined the simulated difference of the meridional circulation induced by the wind QBO (the difference of the residual circulation simulated with the wind QBO from that simulated without it). As mentioned by Chen et al. (2002), the induced difference of the residual circulation consists of three pairs of cells vertically aligned in the range 120 hPa–1.5 hPa (about 15 km–45 km). When the easterly phase of the wind QBO is

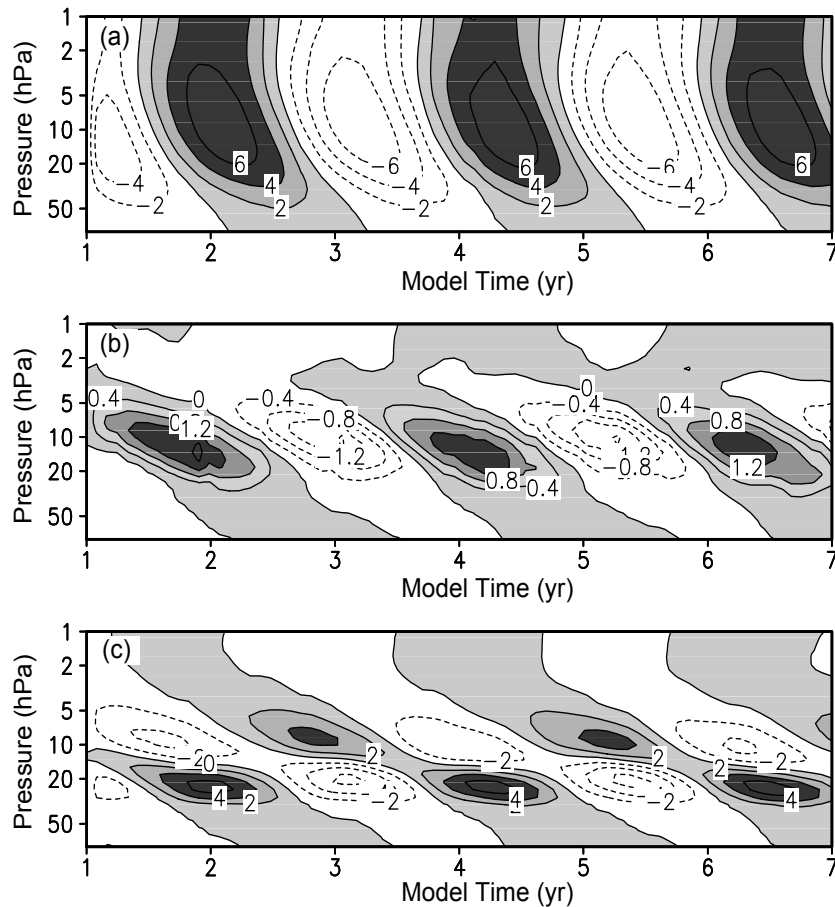


Fig. 5. (a) The wind QBO calculated by the model (units: $m s^{-1}$), (b) simulated HCl QBO (units: 0.1 ppbv), and (c) O_3 QBO (units: 0.1 ppmv) over the equator.

strong, the three pairs of cells are located at the levels below 50 hPa, 50–6 hPa and above 6 hPa, respectively. The cells in the middle are stronger, with the flow moving upward over the equator and splitting to the south and north in the 10 hPa–5 hPa layer. The flow turns downward in the extratropics and flows back to the equator near the 50 hPa level. The cells below 50 hPa and above 5 hPa move in the opposite direction compared with the cells in the 50 hPa–~6 hPa range, as shown by the vectors in Fig. 6a. When the simulation time is increased, the three pairs of cells move down gradually. And during the movement, the middle cells weaken and the upper cells strengthen. When the simulation reaches the next model year with the westerly phase of the wind QBO being strong, the induced cells continue to move down. The original highest altitude cells just replace the middle cells and the original middle cells replace the cells below them. At that time, the locations of the three pairs of cells are almost the same as the locations in the easterly phase of the wind QBO, except the directions of the cells are reversed, as shown in Fig. 6b. The locations of the induced circulation change continuously in cycles when the phase of the wind is changed.

The solid lines in Fig. 6 show that the HCl partial pressure increases with height, and the partial pressure vertical gradient is larger in the layer between 30 hPa and 5 hPa. It can be seen from Fig. 6a that when the easterly phase of the wind QBO dominates, the induced upward flow in the 50–6 hPa range transports the air with lower HCl density upward, causing a decrease in HCl density in the 40 hPa–5 hPa layer.

At the same time, the induced downward flow in the 50 hPa–~6 hPa range over the extratropics transports air with higher HCl density downward. So there is a region where the HCl density increases over the extratropics. Because the vertical gradients of HCl partial pressure below 50 hPa and above 5 hPa over the equator are small, the changes in HCl mixing ratio caused by the wind QBO-induced meridional circulation are small. This explains HCl mixing ratio changes in the easterly phase as shown in Fig. 7a. Since the location of the induced meridional circulation in the westerly phase is the same as that in the easterly phase, while the direction of the induced meridional circulation is opposite for the two phases, the transports in various levels in the westerly phase are reversed. This makes the HCl mixing ratio increase in the 40 hPa–5 hPa layer over the equator and decrease over the extratropics as shown in Fig. 7b.

A prudent question is why the same wind QBO forcing would lead to very different vertical structures for the HCl and O₃ QBOs. This depends on the different vertical density distributions of these two gases. It is well known that the O₃ partial pressure reaches a maximum value near 20 hPa, which then rapidly decreases upward and downward. Due to the effect of the wind QBO-induced meridional circulation, the transports of O₃ in various levels are different from those of HCl (as shown in Fig. 8).

Since the transports of O₃ in different altitudes and latitudes caused by the wind QBO-induced meridional circulation have been described in detail by Chen et al. (2002), we will not repeat the discussion. Here, we

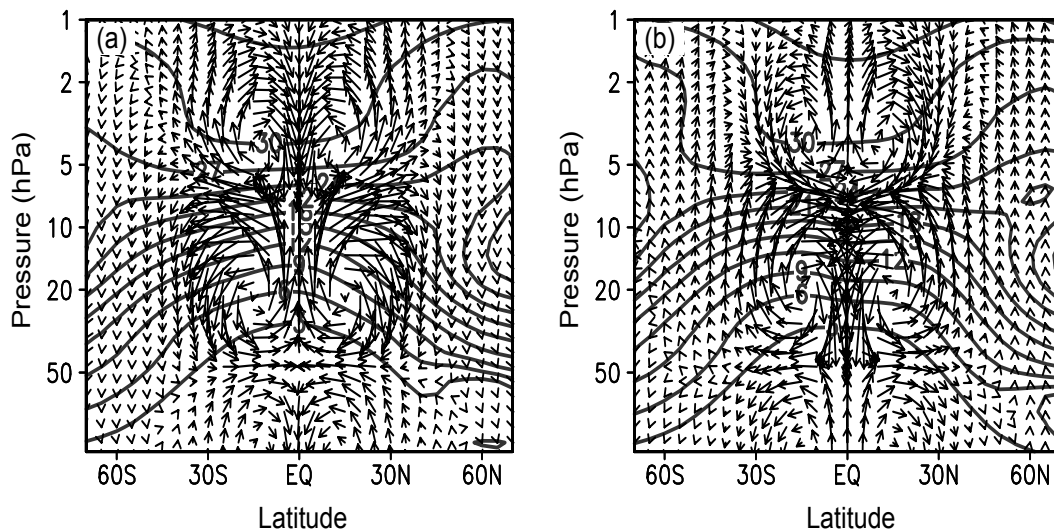


Fig. 6. Simulated wind QBO-induced residual circulation (vectors) (units: m s^{-1} , the vertical wind is magnified 500 times) and HCl partial pressure (contours) (units: 0.1 ppbv). (a) easterly phase; (b) westerly phase.

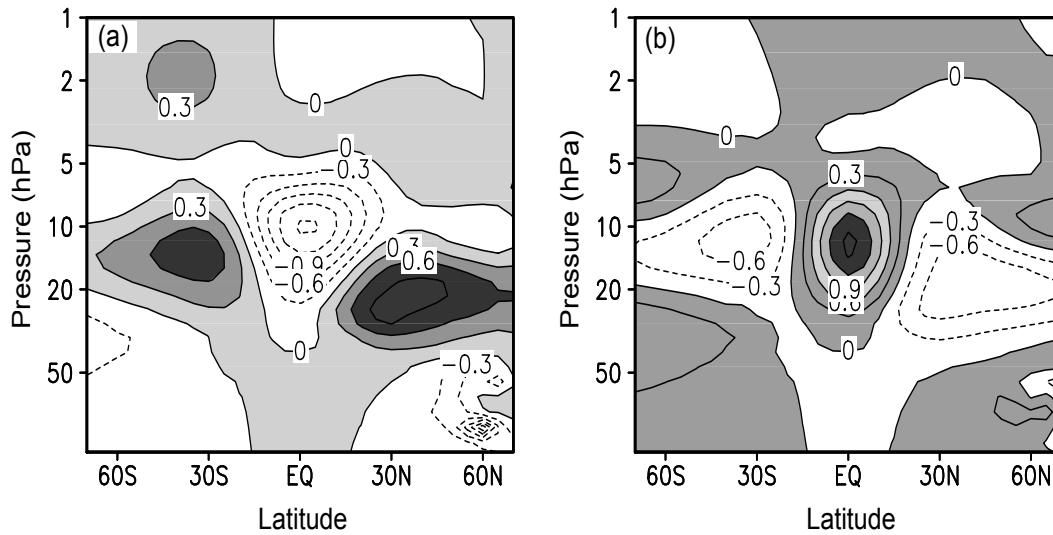


Fig. 7. Simulated latitude-height cross section for the HCl mixing ratio change (0.1 ppbv), (values simulated with the wind QBO minus the values without it). (a) easterly phase; (b) westerly phase.

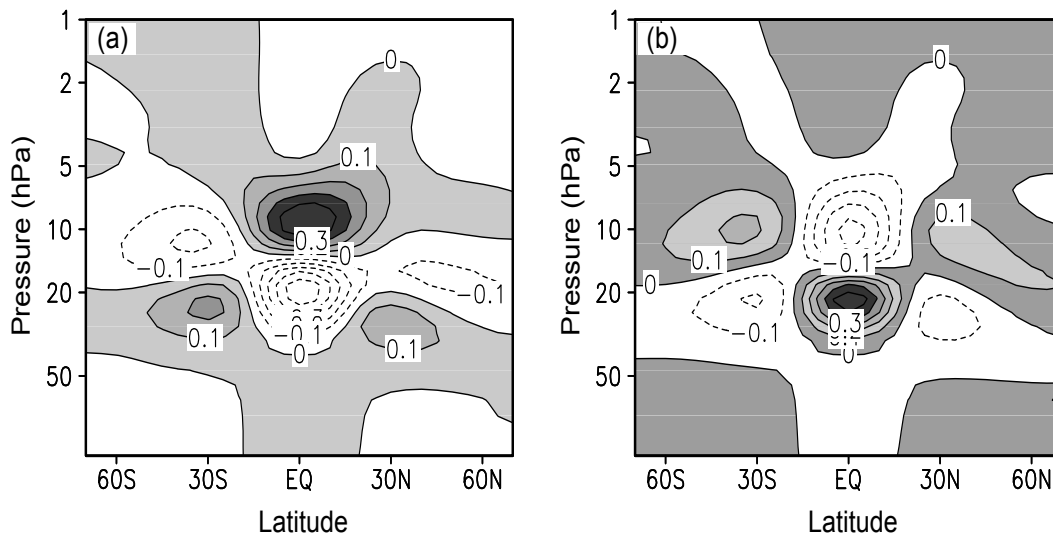


Fig. 8. Simulated latitude-height cross section for the ozone mixing ratio change (1.0 ppmv), (values simulated with the wind QBO minus the values without it). (a) easterly phase; (b) westerly phase.

just discuss the impact of HCl QBO on ozone QBO. Since HCl is a long-lived tracer, its concentration is controlled by dynamic transport in both the upper and lower stratosphere. The chemical time constant for O_x (odd oxygen, including O_3 and O) is long in the lower stratosphere (typically of the order of 10^7 s), so that the ozone QBO signals are mainly dynamically controlled in this range. The O_x chemical time constant is reduced with height in the stratosphere, typically of the order of 10^6 s at the level near 10 hPa, while the dynamical time constant is about 10^7 s in order. So the photochemical processes become important. Com-

paring Fig. 8 with Fig. 7, when the transport of the induced meridional circulation makes the O_3 concentration increase near 10 hPa in easterly phase (or decrease in westerly phase), we see that it makes the HCl concentration decrease in the same region and in the same phase (or increase in westerly phase). Furthermore, in this case, the induced HCl disturbances will destroy less ozone in the easterly phase (or destroy more ozone in the westerly phase). Therefore the dynamically driven HCl QBO will enhance the O_3 QBO in the upper stratosphere through ozone destructive catalysis by HCl.

4. Conclusions

The HCl QBO was analyzed using HALOE data and also simulated using the NCAR two-dimensional interactive chemical, dynamical and radiative model. The results were compared with the ozone QBO. The results show the following.

(1) The QBO signals in HCl mixing ratio occur mainly in the altitude range 50 hPa to 5 hPa; the larger amplitudes are located between 30 hPa and 10 hPa; the higher HCl mixing ratio usually corresponds to the westerly phase of the wind QBO and the lower HCl mixing ratio to the easterly phase in the layer from 50 hPa to 20 hPa. The vertical structure of the HCl QBO is not as complex as the ozone QBO over the equator.

(2) The QBO for HCl and O₃ are almost in phase at the 50 hPa–20 hPa level while they are out of phase near 10 hPa.

(3) The QBO signals for HCl both in the northern and southern hemispheric extratropics are also clear, but the phases are reversed compared with the phase of the tropical QBO. The phases reverse near 12°N/S latitude and show hemispheric asymmetry. The HCl QBO signals in the region between 30°N and 40°N are stronger than those between 30°S and 40°S.

(4) The simulated structures of the HCl QBO agree well with observations, and because the vertical distribution of HCl density is different from that of O₃, the transports of HCl by the wind QBO-induced meridional circulation in various levels are also different.

(5) Since the O₃ and HCl QBOs are out of phase above 10 hPa, and since the chemical time constant for O₃ is much shorter than the dynamical time constant in the middle stratosphere, the dynamically driven HCl QBO will enhance the O₃ QBO in the middle stratosphere through ozone destructive catalysis by HCl. The influence of the HCl QBO on O₃ QBO is not significant in the lower stratosphere.

Acknowledgments. This work was supported by the National Natural Science Foundation of China (Grant No. 40375012) The authors would like to express their thanks to the HALOE Science and Engineering teams who have worked so hard to provide an excellent dataset and to NCAR for providing us with the NCAR two-dimensional interactive chemical, dynamical and radiative model.

REFERENCES

Chen Yuejuan, Zheng Bin, and Zhang Hong, 2002: The features of ozone quasi-biennial oscillation in the trop-

ical stratosphere and its numerical simulation. *Adv. Atmos. Sci.*, **19**(5), 777–793.

Chipperfield, M. P., L. J. Kinnery, and J. Zawodny, 1994: A two-dimensional model study of the QBO signal in SAGE II NO₂ and O₃. *Geophys. Res. Lett.*, **21**, 589–592.

Funk, J. P., and G. L. Garnham. 1962: Australian ozone observations and a suggested 24 month cycle. *Tellus*, **14**, 378–382.

Gray, L. J., and M. P. Chipperfield, 1990: On the interannual variability of trace gases in the middle atmosphere. *Geophys. Res. Lett.*, **17**, 933–936.

Gray, L. J., and S. Ruth, 1992: The interannual variability of trace gases in the stratosphere: A comparative study of the LIMS and UARS measurement periods. *Geophys. Res. Lett.*, **19**, 673–676.

Hasebe, F., 1983, Interannual variations of global ozone revealed from Nimbus 4 UV and ground-based observations. *J. Geophys. Res.*, **88**, 6819–6834.

Huang, T., and Coauthors, 1997: Description of SOCRATES, A chemical, dynamical, radiative 2-D model. Tech. Rept, NCAR, Boulder, Colorado, 88pp.

Luo, M., J. M. Russell III, and T. Y. W. Huang, 1997: Halogen Occultation Experiment observations of the quasi-biennial oscillation and the effects of Pinatubo aerosol in the tropical stratosphere. *J. Geophys. Res.*, **102**, 19187–19198.

Ramanathan, K. R., 1963: Bi-annual variation of atmospheric ozone over the tropics. *Quart. J. Roy. Meteor. Soc.*, **89**, 540–542.

Reed, R. J., W. J. Campbell, L. A. Rasmussen, and D. G. Rogers, 1961: Evidence of downward propagating annual wind reversal in the equatorial Stratosphere. *J. Geophys. Res.*, **66**, 813–818.

Russell, and Coauthors, 1993: The Halogen Occultation Experiment. *J. Geophys. Res.*, **98**(D6), 10777–10797.

Schoeberl, M. R., A. E. Roche, J. M. Russell III, D. Ortland, P. B. Hays, and J. W. Waters, 1997: An estimation of the dynamical isolation of the tropical lower stratosphere using UARS wind and trace gas observations of the quasi-biennial oscillation. *Geophys. Res. Lett.*, **24**, 53–56.

Veryard, R. G., and R. A. Ebdon, 1991: Fluctuation in tropical stratosphere winds. *Meteor. Mag.*, **90**, 125–143.

Yang, H., and K. K. Tung, 1995: On the phase propagation of extratropical ozone quasi-biennial oscillation in observational data. *J. Geophys. Res.*, **100**, 9091–9100.

Zawodny, J. M., and M. P. McCormick, 1991: Stratospheric Aerosol and Gas Experiment II measurements of the quasi-biennial oscillations in ozone and nitrogen dioxide. *J. Geophys. Res.*, **96**, 9371–9377.

Zhang Hong, Chen Yuejuan, and Wu Beiying, 2000: Impact of quasi-biennial oscillation on the distribution of the trace gases in the stratosphere. *Chinese J. Atmos. Sci.*, **24**(1), 103–110.